PHYSICAL REVIEW RESEARCH **5**, L042030 (2023)

Letter

Asymmetric thermal relaxation in driven systems: Rotations go opposite ways

Cai Dieball, Gerrit Wellecke,* and Aljaž Godec†

Mathematical bioPhysics group, Max Planck Institute for Multidisciplinary Sciences, 37077 Göttingen, Germany

(Received 13 April 2023; revised 12 June 2023; accepted 24 October 2023; published 27 November 2023)

It was predicted and recently experimentally confirmed that systems with microscopically reversible dynamics in quadratic potentials warm up faster than they cool down. This thermal relaxation asymmetry challenged our understanding of relaxation far from equilibrium. Because the intuition and proof hinged on the dynamics obeying detailed balance, it was not clear whether the asymmetry persists in systems with irreversible dynamics. To fill this gap, we here prove the relaxation asymmetry for systems driven out of equilibrium by a general linear drift. The asymmetry persists due to a nontrivial isomorphism between driven and reversible processes. Moreover, rotations of level sets of probability densities emerge that, strikingly, occur in opposite directions during heating and cooling. This highlights that noisy systems do not relax by passing through local equilibria.

DOI: 10.1103/PhysRevResearch.5.L042030

Introduction. According to the laws of thermodynamics, systems in contact with a thermal environment evolve to the temperature of their surroundings in the process called thermal relaxation [1]. Relaxation close to equilibrium may be explained by linear response theory conceptually based on Onsager's regression hypothesis [2–4]. That is, relaxation from a temperature quench is indistinguishable from the decay of a spontaneous thermal fluctuation at equilibrium [2–4]. Analogous results were meanwhile formulated also for relaxation near nonequilibrium steady states [5–7]. Beyond the linear regime, however, the regression hypothesis and perturbative arguments fail. In particular, noisy systems do not relax by passing through local equilibria; that is, intermediate states do not correspond to equilibrium states at intermediate temperatures, $p(\mathbf{x},t)\neq p_{\mathrm{eq}}[\mathbf{x};T(t)]$ with a time-dependent temperature $T(t)$.

Important advances have been made in understanding relaxation beyond the linear regime addressing hydrodynamic limits [8,9], barrier crossing in driven systems [10,11], memory effects [12–21], far-from-equilibrium fluctuation-dissipation theorems [22,23], optimal heating or cooling protocols [24], anomalous relaxation also known as the Mpemba effect [25–32] and its isothermal analog [33], the Kovacs effect [34,35], and dynamical phase transitions [36–44]. Important advances further include transient thermodynamic uncertainty relations [45–50], speed limits [51–55], and analyses of relaxation from the viewpoint of information geometry [54–56].

A particularly striking feature of relaxation was unraveled with the discovery of the asymmetry between heating and cooling from thermodynamically equidistant temperature quenches [57]. That is, it was found that systems with locally quadratic energy landscapes and microscopically reversible dynamics heat up faster than they cool down. Later works expanded on this result [58–60]. The asymmetry was recently quantitatively confirmed by experiments [56].

The asymmetry emerges because the entropy production within the system during heating is more efficient than heat dissipation into the environment during cooling [57]. In turn, close to equilibrium they become equivalent and symmetry is restored [56,57]. An even deeper understanding of the asymmetry was recently achieved by means of thermal kinematics [56]. However, both the reasoning and the proof of the asymmetry [56,57,61] seem to hinge on the reversibility of the dynamics. Therefore, the persistence of the asymmetry in systems driven into nonequilibrium steady states (NESS) was unexpected. In particular, a nonconservative force profoundly changes relaxation behavior [62–66] even near stable fixed points [67] and in systems with linear drift [68], and may thus *a priori* also break the asymmetry.

Here, we investigate the speed and asymmetry of thermal relaxation to a NESS. As a paradigmatic example we first consider a harmonically confined Rouse polymer with hydrodynamic interactions and internal friction driven by shear flow (see Fig. 1), and demonstrate that heating is faster than cooling. Next we provide a systematic analysis of relaxation under broken detailed balance and explain under which conditions heating and cooling both become faster. Finally, we prove that all ergodic systems with a linear drift, including those driven arbitrarily far from equilibrium and displaying rotational motions, heat up faster than they cool down. In this regime the notion of a local effective nonequilibrium temperature is nominally impossible. Our proof, which exploits dual-reversal symmetry, unravels a nontrivial isomorphism

*Present address: Theory of Biological Fluids, Max Planck Institute for Dynamics and Self-Organization, 37077 Göttingen, Germany.

†agodec@mpinat.mpg.de

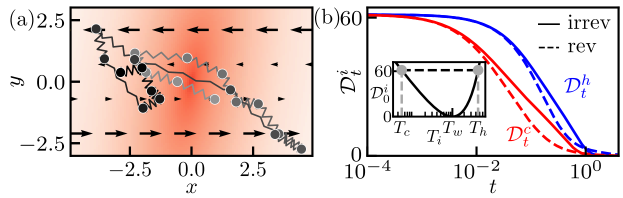

FIG. 1. (a) Configuration of a harmonically confined (color gradient) Rouse polymer with $N = 20$ beads in three dimensions with hydrodynamic interactions and internal friction subject to a shear flow (arrows) in the x-y plane drawn from the NESS with covariance $\mathbf{\Sigma}_{s,w}$ (see Ref. [69] for parameters); a projection onto the x-y plane is shown. (b) The corresponding free energy difference $\mathcal{D}_t^i$ in Eq. (5) during heating from T_c (red) and cooling from T_h (blue) with (solid lines) and without (dashed lines) irreversible shear flow. The shear changes $\mathcal{D}_t^i$, but the thermal relaxation asymmetry $\mathcal{D}_t^c < \mathcal{D}_t^h$ for $t > 0$ remains valid. Inset: Temperatures T_i before the quench are chosen thermodynamically equidistant, i.e., $\mathcal{D}_0^c = \mathcal{D}_0^h$.

between reversible and driven systems. Finally, we find an unexpected facet of the relaxation asymmetry—effective rotations of probability densities occur in opposite directions during heating and cooling, respectively.

Setup and motivating example. The relaxation asymmetry was originally proven for reversible diffusions in locally quadratic energy landscapes as well as their low-dimensional projections [57,61]. It states that such systems, when quenched from thermodynamically equidistant (TED) temperatures T_h, T_c to an ambient temperature T_w with $T_c < T_w < T_h$, heat up faster than they cool down. In quantitative terms, for degrees of freedom $\mathbf{x}$ (e.g., positions) at time t, the generalized excess free energy in units of $k_\mathrm{B}T_w$ [67,70–72] or nonadiabatic entropy production [73,74] (i.e., the relative entropy in units of k_B [75] between the instantaneous $P_i^w(\mathbf{x},t)$ and stationary $p_\mathrm{s}^w(\mathbf{x})$ probability density at T_w with $i = h, c$)

$$\mathcal{D}_t^i \equiv \mathcal{D}_\mathrm{KL}\left[P_i^w(\mathbf{x},t)||p_\mathrm{s}^w(\mathbf{x})\right] \equiv \int d\mathbf{x} P_i^w(\mathbf{x},t)\ln\frac{P_i^w(\mathbf{x},t)}{p_\mathrm{s}^w(\mathbf{x})}, \tag{1}$$

is always smaller during heating [57,61]. That is, $\mathcal{D}_t^c < \mathcal{D}_t^h$ for all $t > 0$ and all TED T_h and T_c.

In a strict sense, the asymmetry is to be understood as a statement about linearized drift around a local minimum in some high-dimensional energy landscape [57]; counterexamples for diffusion in rugged landscapes [57] and for small quenches also in sufficiently anharmonic wells [60] are known. The generalization to driven systems therefore involves a linear drift that, however, does not derive from a potential and breaks detailed balance. Our main result is the discovery and proof (see last section) of the asymmetry $\mathcal{D}_t^c < \mathcal{D}_t^h$ in driven systems.

Consider a d-dimensional system evolving according to the overdamped Langevin equation [76,77]

$$d\mathbf{x}_t = -\mathbf{A}\mathbf{x}_t dt + \boldsymbol{\sigma}_i d\mathbf{W}_t, \tag{2}$$

with square drift and noise-amplitude matrices, $\mathbf{A}$ and $\boldsymbol{\sigma}_i$, respectively. In terms of the friction matrix $\boldsymbol{\gamma}$, given by Stokes' law, the positive definite diffusion matrix reads $\mathbf{D}_i \equiv \boldsymbol{\sigma}_i\boldsymbol{\sigma}_i^T/2 = k_B T_i \boldsymbol{\gamma}^{-1}$ and thus depends linearly on temperature T_i. The external force $\mathbf{F}(\mathbf{x})$ yields a T_i-independent drift $-\mathbf{A}\mathbf{x} = \boldsymbol{\gamma}^{-1}\mathbf{F}(\mathbf{x})$, where $\mathbf{A}$ is generally nonsymmetric but confining, i.e., the eigenvalues of $\mathbf{A}$ have positive real parts. Thus, $\mathbf{x}_t$ is ergodic but irreversible with zero-mean Gaussian NESS density $p_\mathrm{s}^i(\mathbf{x}) = (2\pi)^{-d/2}\det[\mathbf{\Sigma}_{\mathrm{s},i}]^{-1/2}\exp[-\mathbf{x}^T\mathbf{\Sigma}_{\mathrm{s},i}^{-1}\mathbf{x}/2]$ where the covariance $\mathbf{\Sigma}_{\mathrm{s},i}$ obeys the Lyapunov equation [69]

$$\mathbf{A}\mathbf{\Sigma}_{\mathrm{s},i} + \mathbf{\Sigma}_{\mathrm{s},i}\mathbf{A}^T = 2\mathbf{D}_i = 2k_B T_i\boldsymbol{\gamma}^{-1}, \tag{3}$$

and thus depends linearly on the temperature T_i. Equation (3) implies for all T_i the decomposition into reversible $-\mathbf{A}_\mathrm{rev}\mathbf{x} \equiv \mathbf{D}_i\nabla\ln p_\mathrm{s}^i(\mathbf{x}) = -\mathbf{D}_i\mathbf{\Sigma}_{\mathrm{s},i}^{-1}\mathbf{x}$ and irreversible $-\mathbf{A}_\mathrm{irr}\mathbf{x} \equiv (-\mathbf{A}+\mathbf{A}_\mathrm{rev})\mathbf{x} = -\boldsymbol{\alpha}_i\mathbf{\Sigma}_{\mathrm{s},i}^{-1}\mathbf{x}$ drift [78], where $\boldsymbol{\alpha}_i^T = -\boldsymbol{\alpha}_i$ is an antisymmetric matrix.[1]

We focus on temperature quenches—instantaneous changes of the environmental temperature at fixed drift. The thermodynamics of relaxation upon a quench $T_i \to T_w$ is fully specified by $\mathcal{D}_t^i$, as the adiabatic entropy production (housekeeping heat divided by T_w) [74] merely embodies the cost of maintaining the NESS [79] and thus need not be considered. Therefore, TED temperatures $T_{h,c}$ correspond to $\mathcal{D}_0^h = \mathcal{D}_0^c$ and are equal to those of a reversible system at the same T_w [57].

Since the initial condition is a zero-mean Gaussian with $\mathbf{\Sigma}_i^w(0) = \mathbf{\Sigma}_{\mathrm{s},i}$, the probability density is Gaussian for all times with $\mathbf{\Sigma}_i^w(t) \equiv \langle\mathbf{x}_t\mathbf{x}_t^T\rangle_i^w - \langle\mathbf{x}_t\rangle_i^w\langle\mathbf{x}_t^T\rangle_i^w$ given by (see Supplemental Material [69])

$$\frac{d}{dt}\mathbf{\Sigma}_i^w(t) = -\mathbf{A}\mathbf{\Sigma}_i^w(t) - \mathbf{\Sigma}_i^w(t)\mathbf{A}^T + 2\mathbf{D}_w$$
$$\Rightarrow \mathbf{\Sigma}_i^w(t) = \mathbf{\Sigma}_{\mathrm{s},w} + \mathrm{e}^{-\mathbf{A}t}[\mathbf{\Sigma}_{\mathrm{s},i} - \mathbf{\Sigma}_{\mathrm{s},w}]\mathrm{e}^{-\mathbf{A}^T t}, \tag{4}$$

where $\langle\cdot\rangle_i^w$ denotes the average over all paths $\mathbf{x}_t$ at temperature T_w evolving from $p_\mathrm{s}^i(\mathbf{x})$. Note that $\mathbf{\Sigma}_{\mathrm{s},i} = T_i\mathbf{\Sigma}_{\mathrm{s},w}/T_w$ [see Eq. (3)]. Introducing $\delta\tilde{T}_i \equiv T_i/T_w - 1$, the generalized excess free energy reads (see Ref. [69])

$$\mathcal{D}_t^i = \tfrac{1}{2}\delta\tilde{T}_i\,\mathrm{tr}\mathbf{X}(t) - \tfrac{1}{2}\ln\det[\mathbb{1} + \delta\tilde{T}_i\mathbf{X}(t)], \tag{5}$$

where we introduced the $d \times d$ matrix

$$\mathbf{X}(t) \equiv \mathrm{e}^{-\mathbf{A}t}\mathbf{\Sigma}_{\mathrm{s},w}\mathrm{e}^{-\mathbf{A}^T t}\mathbf{\Sigma}_{\mathrm{s},w}^{-1}, \tag{6}$$

which via Eq. (5) fully describes relaxation dynamics.

As a paradigmatic example for such processes we consider a harmonically confined Rouse polymer with N beads experiencing hydrodynamic interactions [80,81] and internal friction [82–85] subject to a shear flow, which was investigated experimentally in Refs. [86–94]. For a representative configuration of the NESS ensemble, see Fig. 1(a). One may also consider colloidal particles in the presence of nonconservative optical forces [95]. The effect of these forces is included in the $3N \times 3N$ drift matrix $\mathbf{A}$ and $3N \times 3N$ noise amplitude $\boldsymbol{\sigma}_i$ [69]. Evaluating $\mathcal{D}_t^i$ for the heating and cooling processes upon quenches from TED temperatures T_h and T_c we find $\mathcal{D}_t^c < \mathcal{D}_t^h$ for all $t > 0$. That is, heating is faster than

[1]As $\mathbf{\Sigma}_{\mathrm{s},i}$ is invertible and symmetric Eq. (3) implies $\boldsymbol{\alpha}_i = (\mathbf{A} - \mathbf{D}_i\mathbf{\Sigma}_{\mathrm{s},i}^{-1})\mathbf{\Sigma}_{\mathrm{s},i} = -\mathbf{\Sigma}_{\mathrm{s},i}(\mathbf{A}^T - \mathbf{\Sigma}_{\mathrm{s},i}^{-1}\mathbf{D}_i) = -\boldsymbol{\alpha}_i^T$. In fact $\mathbf{\Sigma}_{\mathrm{s},i}^{-1}\mathbf{x}$ and $\boldsymbol{\alpha}_i\mathbf{\Sigma}_{\mathrm{s},i}^{-1}\mathbf{x}$ are orthogonal since their scalar product yields an antisymmetric quadratic form $\mathbf{x}^T\mathbf{\Sigma}_{\mathrm{s},i}^{-1}\boldsymbol{\alpha}_i\mathbf{\Sigma}_{\mathrm{s},i}^{-1}\mathbf{x} = 0$ [67].

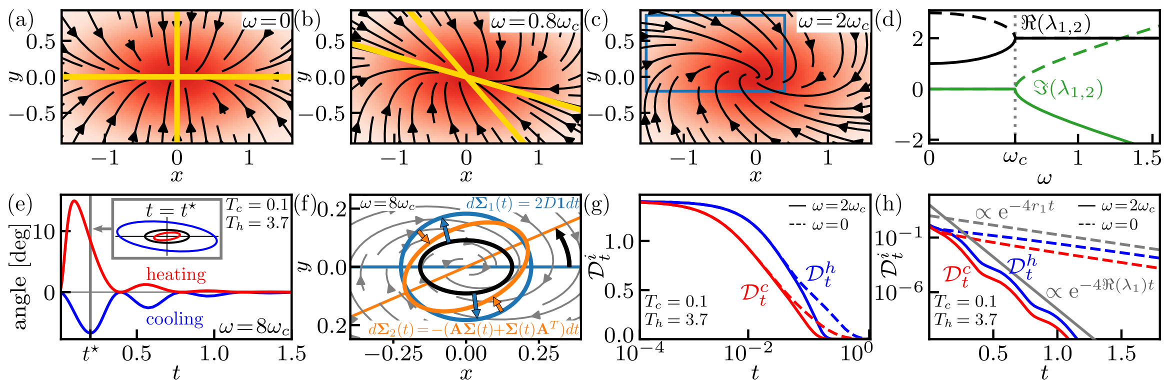

FIG. 2. (a)–(c) Steady-state density $p_s^w(\mathbf{x})$ (color gradient) and streamlines of the drift field $-\mathbf{A}\mathbf{x}$ for a two-dimensional motion in Eq. (2) with $\boldsymbol{\sigma}_w=\sqrt{2}\mathbb{1}$ and drift matrix $\mathbf{A}$ with elements $A_{jj}=r_j$ with $r_1=1$, $r_2=3$, $A_{jk}=(-1)^j\omega r_k$ for $j,k\in\{1,2\}$, with ω in units of $\omega_c\equiv|r_2-r_1|/2\sqrt{r_1r_2}$. Real eigendirections (yellow) only exist for $\omega\leqslant\omega_c$. (d) Real and imaginary parts of eigenvalues of $\mathbf{A}$ as a function of ω. At $\omega=\omega_c$ the eigenvalues coincide and eigendirections [yellow lines in (b), (c)] merge, i.e., $\mathbf{A}$ is not diagonalizable. For $\omega>\omega_c$ the eigenvalues are complex. (e) Angle between the principal axes of the covariance matrices $\boldsymbol{\Sigma}_i^w(t)$ and $\boldsymbol{\Sigma}_{s,w}$ reflecting the rotation of level sets of the Gaussian probability densities. (f) Explanation of the counterintuitive opposing effective rotations at small times during heating from $T_c/T_w=0.1$. The change $d\boldsymbol{\Sigma}(t)$ in Eq. (4) starting from the initial $\boldsymbol{\Sigma}_{s,i}$ (black ellipse) for $dt=0.05$ split into diffusive (yielding the blue ellipse) and drift along the gray streamlines (yielding orange ellipse) contributions. (g)–(h) $\mathcal{D}_t^i$ for heating and cooling with and without driving on logarithmic-linear and linear-logarithmic scales. The driven system relaxes faster at large t as predicted from the eigenvalues in (e). Gray lines in (h) show the limiting relaxation rates for long times, e^{-4r_1t} (dashed line) and $e^{-4\Re(\lambda_1)t}$ (solid line).

cooling [the red line in Fig. 1(b) is at all times below the blue line]. This agrees with the relaxation asymmetry predicted [57] and experimentally verified [56] in reversible systems, and provokes the question if this holds for any linear driving.

Systematics of breaking detailed balance. We now systematically assess the influence of nonequilibrium drifts on relaxation upon a temperature quench. As shown above, any linear drift $\mathbf{A}$ for $i=c,w,h$ decomposes as

$$\mathbf{A}=(\mathbf{D}_i+\boldsymbol{\alpha}_i)\boldsymbol{\Sigma}_{s,i}^{-1}\quad\text{with}\quad\boldsymbol{\alpha}_i^{\mathrm{T}}=-\boldsymbol{\alpha}_i.\tag{7}$$

Thus, by choosing any antisymmetric matrix $\boldsymbol{\alpha}_i$ we alter the NESS current as well as $\mathbf{X}(t)$, but neither $\boldsymbol{\Sigma}_{s,i}$ nor $p_s(\mathbf{x})$. We can thus directly compare a NESS with the corresponding reversible system $\boldsymbol{\alpha}_i=\mathbf{0}$ with the same steady state. Note that such a direct comparison is not given in the example in Fig. 1, since the shear flow alters $\boldsymbol{\Sigma}_{s,i}$ as it is not of the form $\boldsymbol{\alpha}_i\boldsymbol{\Sigma}_{s,i}^{-1}$ with $\boldsymbol{\alpha}_i^T=-\boldsymbol{\alpha}_i$ (see Ref. [69] for details about the consistent comparison of equilibrium versus nonequilibrium).

We now consider the influence of the nonequilibrium driving. For linear drift the relaxation is governed by the eigenvalues of $\mathbf{A}$ [96,97]. Since $\boldsymbol{\Sigma}_{s,i}$ is, by definition, symmetric with positive eigenvalues, we can find a matrix $\boldsymbol{\beta}=\boldsymbol{\beta}^T$ such that $\boldsymbol{\beta}^2\equiv\boldsymbol{\Sigma}_{s,i}^{-1}$.[2] Thus, the matrix $\boldsymbol{\beta}\mathbf{D}_i\boldsymbol{\Sigma}_{s,i}^{-1}\boldsymbol{\beta}^{-1}=\boldsymbol{\beta}\mathbf{D}_i\boldsymbol{\beta}=\boldsymbol{\beta}\boldsymbol{\sigma}_i(\boldsymbol{\beta}\boldsymbol{\sigma}_i)^T/2$ is symmetric, which alongside $\det(\boldsymbol{\beta}\boldsymbol{\sigma}_i)\neq0$ implies that $\mathbf{D}_i\boldsymbol{\Sigma}_{s,i}^{-1}$ is diagonalizable with positive eigenvalues.[3] Therefore, in the absence of driving $\mathbf{A}=\mathbf{D}_i\boldsymbol{\Sigma}_{s,i}^{-1}$ expectedly has strictly positive eigenvalues reflecting a monotonous relaxation to equilibrium.

Once we include driving $\boldsymbol{\alpha}_w\neq0$ in the steady-state-preserving form Eq. (7), the spectrum may or may not become complex depending on the detailed form of $\boldsymbol{\alpha}_w$, see, e.g., Figs. 2(a)–2(d). Complex eigenvectors imply that eigendirections where the drift points straight towards $\mathbf{0}$ cease to exist, see Figs. 2(a)–2(c). This happens already at arbitrarily small driving if level sets of $p_s(\mathbf{x})$ are (hyper)spherical. If some eigenvalues are on the threshold of becoming complex [branching point ω_c in Fig. 2(d)], $\mathbf{A}$ may become nondiagonalizable. In terms of the minimal 2D example in Fig. 2 we have that $\mathbf{A}$ is nondiagonalizable when $\omega=\pm\omega_c$ [see Fig. 2(d)].

An interesting consequence of driving is that the different dimensions no longer decouple as they do under detailed balance [see Fig. 2(a)]. This means that the d-dimensional Langevin equation (2) cannot be decomposed into 1D equations and that rotational dynamics may emerge. In the particular case of temperature quenches we find that driving causes a time-dependent rotation of the level sets of $P_i^w(\mathbf{x},t)$, see Fig. 2(e). In agreement with the opposite signs of T_i-T_w in Eq. (4), these rotations occur in opposite directions during heating and cooling, which is a striking feature of the relaxation asymmetry. These rotations further underscore that thermal relaxation must not be understood as passing through local equilibria at intermediate (effective) temperatures (since these would not be rotated with respect to the steady-state density), and that heating and cooling here evolve along very distinct pathways in the space of probability distributions (for related statements without rotations see Ref. [56]).

While the initial rotation during cooling follows the direction of driving, most surprisingly the effective rotations during heating initially oppose the direction of the driving [see Fig. 2(e)]. This effect can be traced to the interplay of (Trotterized [98]) diffusion and drift during individual small time increments, see Fig. 2(f). During heating for an increment dt diffusion alone propagates the black to the more circular blue ellipse. The subsequent drift along the

[2] From the orthogonal diagonalization $\mathbf{O}\boldsymbol{\Sigma}_{s,i}^{-1}\mathbf{O}^T=\mathrm{diag}(s_j)$ we define $\boldsymbol{\beta}\equiv\mathbf{O}^T\mathrm{diag}\sqrt{s_j}\mathbf{O}$.

[3] Any matrix of the form $\mathbf{M}\mathbf{M}^T$ is symmetric, and therefore diagonalizable, with real non-negative eigenvalues, since $\mathbf{M}\mathbf{M}^T\mathbf{v}=\lambda\mathbf{v}$ implies $\lambda=\mathbf{v}^T\mathbf{M}\mathbf{M}^T\mathbf{v}/\mathbf{v}^T\mathbf{v}=(\mathbf{M}^T\mathbf{v})^T\mathbf{M}^T\mathbf{v}/\mathbf{v}^T\mathbf{v}\geqslant0$.

elliptical streamlines propagates this blue ellipse to the orange ellipse that is, however, effectively rotated in the direction opposite to the drift (for further details see Ref. [69]). During the initial step of cooling, this does not happen since the diffusion becomes negligible compared to the drift, and the shape becomes less round even for short times, see Fig. S3 in Ref. [69]. In higher dimensions we observe opposing rotations in two-dimensional subspaces, see Fig. S5 in Ref. [69] for the example of a sheared Rouse polymer.

Accelerated relaxation. Before proving the relaxation asymmetry we discuss the acceleration of relaxation via driving [64–66,68]. We therefore focus on the real part of the eigenvalues, which determines the relaxation timescales. Upon a change of basis we find $\widetilde{\mathbf{A}} \equiv \boldsymbol{\beta}\mathbf{A}\boldsymbol{\beta}^{-1} = \boldsymbol{\beta}\mathbf{D}_i\boldsymbol{\beta} + \boldsymbol{\beta}\boldsymbol{\alpha}_i\boldsymbol{\beta}$ where $(\boldsymbol{\beta}\boldsymbol{\alpha}_i\boldsymbol{\beta})^T = -\boldsymbol{\beta}\boldsymbol{\alpha}_i\boldsymbol{\beta}$. Then, for any complex eigenvalue λ of $\widetilde{\mathbf{A}}$ with eigenvector $\mathbf{v} \neq 0$ we may write $2\Re(\lambda)\mathbf{v}^\dagger\mathbf{v} = (\lambda+\lambda^\dagger)\mathbf{v}^\dagger\mathbf{v} = \mathbf{v}^\dagger(\widetilde{\mathbf{A}}+\widetilde{\mathbf{A}}^\dagger)\mathbf{v} = 2\mathbf{v}^\dagger\boldsymbol{\beta}\mathbf{D}_i\boldsymbol{\beta}\mathbf{v}$, where $\dagger$ denotes the Hermitian adjoint. Decomposing $\mathbf{v}, \mathbf{v}^\dagger$ in the orthonormal eigenbasis of $\boldsymbol{\beta}\mathbf{D}_i\boldsymbol{\beta}$ with eigenvalues $0 < \mu_1 \leqslant \cdots \leqslant \mu_d$, we have with $c_j \in \mathbb{C}$

$$\Re(\lambda) = \frac{\mathbf{v}^\dagger\boldsymbol{\beta}\mathbf{D}_i\boldsymbol{\beta}\mathbf{v}}{\mathbf{v}^\dagger\mathbf{v}} = \frac{\sum_{j=1}^d c_j^\dagger c_j\mu_j}{\sum_{j=1}^d c_j^\dagger c_j} \in [\mu_1, \mu_d]. \tag{8}$$

This means that the real parts of the eigenvalues in the presence of driving remain not only positive, as required for the existence of a steady state, but even remain in the interval $[\mu_1, \mu_d]$. Thus, Eq. (8) states that the smallest real part of eigenvalues of $\mathbf{A}$ under driving obeys $\Re(\lambda_1) \geqslant \mu_1$. Note that $\Re(\lambda_1)$ typically[4] sets the slowest relaxation rate [96,97]. Since $\Re(\lambda_1)$ increases (or does not decrease) upon driving, the latter typically enhances relaxation on long time scales, as already shown in Ref. [68].

Driving also affects the adiabatic entropy production. This effect, however, scales trivially, as the adiabatic entropy production increases with increasing $\boldsymbol{\alpha}_i$ according to $\boldsymbol{\alpha}_i^T\mathbf{D}_i^{-1}\boldsymbol{\alpha}_i$ [69]. Hence, there is no direct connection between faster relaxation and steady-state dissipation, as the influence of driving on the eigenvalues is specific. For example, the acceleration in $d = 2$ saturates [see $\Re(\lambda_1)$ in Fig. 2(d)]. More drastically, multiplying $\boldsymbol{\alpha}_i$ by a factor larger than 1 in $d = 3$ may decrease $\Re(\lambda_1)$ [68].

We see from Eq. (6) that $\mathbf{X}(t) \sim \mathrm{e}^{-2\Re(\lambda_1)t}$ for long times and therefore $\mathcal{D}_t^i \sim \mathrm{e}^{-4\Re(\lambda_1)t}$ [see Ref. [69] and Figs. 2(g)–2(h)]. The statement accelerated relaxation, $\Re(\lambda_1) \geqslant \mu_1$, means that both, heating and cooling will at long times be faster. In general the difference between heating and cooling upon driving can become larger or smaller than for reversible dynamics with the same $\boldsymbol{\Sigma}_{s,i}$, but as we now prove heating is always faster than cooling.

Proof of relaxation asymmetry in driven systems. We now prove the relaxation asymmetry for the dynamics in Eq. (2), i.e., $\Delta\mathcal{D}_t \equiv \mathcal{D}_t^h - \mathcal{D}_t^c > 0$ for all $t > 0$. By Eq. (6)

$$\Delta\mathcal{D}_t = \frac{\delta\tilde{T}_h - \delta\tilde{T}_c}{2}\,\mathrm{tr}\mathbf{X}(t) - \frac{1}{2}\ln\frac{\det[\mathbb{1} + \delta\tilde{T}_h\mathbf{X}(t)]}{\det[\mathbb{1} + \delta\tilde{T}_c\mathbf{X}(t)]}. \tag{9}$$

[4]Unless the initial distribution has only a negligible projection onto the slowest modes.

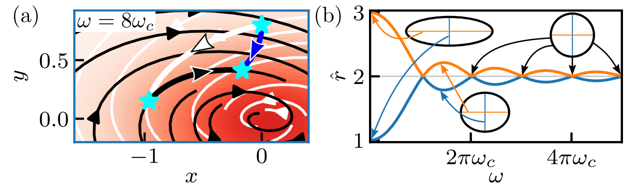

FIG. 3. (a) Illustration of Eq. (10): Stream plot of the drift field $-\mathbf{A}\mathbf{x}$ (black) as in blue frame in Fig. 2(c), and inverted drift field $-\mathbf{A}_{-\boldsymbol{\alpha}}\mathbf{x}$ (white). The white line depicts $\mathrm{e}^{-\mathbf{A}_{-\boldsymbol{\alpha}}\tau}\mathbf{x}_0$ for $\tau \in [0, t]$, the black line is $\mathrm{e}^{-\mathbf{A}\tau}\mathrm{e}^{-\mathbf{A}_{-\boldsymbol{\alpha}}t}\mathbf{x}_0$, and the blue line shows $\mathbf{X}(\tau)\mathbf{x}_0$. (b) Effective stiffness $\hat{r}_j(\omega) \equiv -\ln(x_j^t)/2t$ at $t = 1$ as a function of driving ω (see Ref. [69]). For large driving the directions mix, such that the system effectively approaches a circular parabola with stiffness $(r_1 + r_2)/2$, which is the real part of eigenvalues in Fig. 2(d).

To prove the asymmetry we must understand the properties of $\mathbf{X}(t)$, which is T_i independent. Using the steady-state Lyapunov equation (3) we can rewrite $\mathbf{X}(t)$ as

$$\mathbf{X}(t) = \mathrm{e}^{-\mathbf{A}t}\mathrm{e}^{-\mathbf{A}_{-\alpha}t}, \tag{10}$$

where $\mathbf{A}_{-\boldsymbol{\alpha}} \equiv (\mathbf{D}_w - \boldsymbol{\alpha}_w)\boldsymbol{\Sigma}_{s,w}^{-1}$ is the driving-reversed version of $\mathbf{A}$ as in Eq. (7). This form is reminiscent of the dual-reversal symmetry [78,99–101] stating that time reversal in nonequilibrium steady states requires concurrent current reversal. Equation (10) is illustrated in Fig. 3(a). The proof again requires us to change the basis via $\boldsymbol{\beta}$ as

$$\widetilde{\mathbf{X}}(t) \equiv \boldsymbol{\beta}\mathbf{X}(t)\boldsymbol{\beta}^{-1} = \mathrm{e}^{-\widetilde{\mathbf{A}}t}(\mathrm{e}^{-\widetilde{\mathbf{A}}t})^T, \tag{11}$$

where we used $\boldsymbol{\beta}\mathbf{A}_{-\alpha}\boldsymbol{\beta}^{-1} = \widetilde{\mathbf{A}}^T$ and $\mathrm{e}^{-\widetilde{\mathbf{A}}^Tt} = (\mathrm{e}^{-\widetilde{\mathbf{A}}t})^T$. Thus, $\widetilde{\mathbf{X}}(t)$ is symmetric and hence diagonalizable with real eigenvalues. Since, $\det\mathrm{e}^{-\widetilde{\mathbf{A}}t} = \mathrm{e}^{-\mathrm{tr}\widetilde{\mathbf{A}}t}$, we have $\det\widetilde{\mathbf{X}}(t) = \mathrm{e}^{-2\mathrm{tr}\widetilde{\mathbf{A}}t} \neq 0$. Therefore, $\widetilde{\mathbf{X}}(t)$ and thus $\mathbf{X}(t)$ have positive eigenvalues $x_j^t > 0$, $j = 1, \ldots, d$.[3] Although $\mathbf{A}$ may have complex eigenvalues or even be nondiagonalizable and $\exp(-\mathbf{A}t)$ may be rotational [see Figs. 2(c) and 3(a)], $\mathbf{X}(t)$ has a real eigensystem since consecutive rotations in forward and current-reversed directions effectively cancel rotations, see Eq. (10) and Fig. 3(a).

Using the eigenvalues $x_j^t > 0$ we rewrite Eq. (9) as

$$\Delta\mathcal{D}_t = \sum_{j=1}^d\left(\frac{\delta\tilde{T}_h - \delta\tilde{T}_c}{2}x_j^t - \frac{1}{2}\ln\left[\frac{1+\delta\tilde{T}_hx_j^t}{1+\delta\tilde{T}_cx_j^t}\right]\right). \tag{12}$$

If all $x_j^t \in (0, 1)$, the proof for reversible systems [57,61] asserts that $\Delta\mathcal{D}_t > 0$. It therefore suffices to show that $x_j^t < 1$ for all j, which is equivalent to $||\mathbf{X}(t)|| < 1$, where $||\mathbf{M}|| \equiv \sup_{\mathbf{v}\in\mathbb{R}^d\setminus\mathbf{0}}||\mathbf{M}\mathbf{v}||_2/||\mathbf{v}||_2$ and $||\mathbf{v}||_2 = \sqrt{\mathbf{v}^T\mathbf{v}}$ are the matrix and Euclidean norm, respectively. Equation (10) does not help in showing this;[5] although eigenvalues of $\mathbf{A}$ have positive real parts [see Eq. (8)], it may be that $||\mathrm{e}^{-\mathbf{A}_{\pm\alpha}t}|| > 1$ [e.g., the distance to $\mathbf{0}$ in Fig. 3(a) increases along the white line]. This is possible because the eigenvectors of $\mathbf{A}$ are not orthogonal.

[5]Equation (10) suffices only at equilibrium $\mathbf{A} = \mathbf{A}_{-\boldsymbol{\alpha}} = \mathbf{D}_w\boldsymbol{\Sigma}_{s,w}^{-1}$ where $\mathbf{X}(t) = \exp(-2\mathbf{D}_w\boldsymbol{\Sigma}_{s,w}^{-1}t)$ decomposes into $x_j^t = \exp(-2\mu_jt) < 1$.

We thus change the basis as in Eq. (11) and use the log-norm inequality $||\exp(\mathbf{M}t)|| \leqslant \exp[\mu(\mathbf{M})t]$ [102] with log norm $\mu(\mathbf{M}) \equiv \lim_{h\to 0^+} h^{-1}(||\mathbb{1} + h\mathbf{M}|| - 1)$ yielding $\mu(-\widetilde{\mathbf{A}}) \equiv \mu(-\boldsymbol{\beta}\mathbf{A}\boldsymbol{\beta}^{-1}) = \mu(-\boldsymbol{\beta}\mathbf{D}_w\boldsymbol{\beta}) = -\mu_1$ determined by the symmetric part $(\widetilde{\mathbf{A}} + \widetilde{\mathbf{A}}^T)/2 = \boldsymbol{\beta}\mathbf{D}_w\boldsymbol{\beta}$ [69]. This basis is appropriate because $\boldsymbol{\beta}\boldsymbol{\alpha}_w\boldsymbol{\beta}$ in $\widetilde{\mathbf{A}}$ (unlike $\boldsymbol{\alpha}_w\boldsymbol{\Sigma}_{s,w}^{-1}$ in $\mathbf{A}$) has no symmetric part, i.e., % the driving only affects the rotational part. The log-norm inequality thus implies $||\exp(-\widetilde{\mathbf{A}}t)|| \leqslant \exp[\mu(-\widetilde{\mathbf{A}})t] = \exp(-\mu_1 t)$ and similarly $||\exp(-\widetilde{\mathbf{A}}^T t)|| \leqslant \exp(-\mu_1 t)$, and by the submultiplicative property of the matrix norm we obtain from Eq. (11)

$$||\widetilde{\mathbf{X}}(t)|| \leqslant ||\mathrm{e}^{-\widetilde{\mathbf{A}}t}||\,||(\mathrm{e}^{-\widetilde{\mathbf{A}}t})^T|| \leqslant \mathrm{e}^{-2\mu_1 t} < 1. \tag{13}$$

Since $||\widetilde{\mathbf{X}}(t)|| = ||\mathbf{X}(t)||$ this implies $x_j^t < 1$ and with Eq. (12) completes the proof of $\Delta\mathcal{D}_t > 0$ for all $t > 0$.

The proof provides important insight into the thermodynamics of the asymmetry in reversible versus driven systems. Namely, $\Delta\mathcal{D}_t$ in Eq. (12) for a driven system at any t is equal to that of any reversible system with drift matrix $\hat{\mathbf{A}}$ having eigenvalues $\hat{\mu}_i$ satisfying $\mathrm{e}^{-2\hat{\mu}_j t} = x_j^t$. Therefore, at each t the relaxation asymmetry of a driven system is isomorphic to that of an equilibrium system with different geometry [see Fig. 3(b) for effective stiffness axes of the two-dimensional parabolic potential], which implies the persistence of the asymmetry. This provokes intriguing questions about the existence of the asymmetry in the presence of time-dependent driving.

Conclusion. We have proven that overdamped ergodic systems driven by linear drift, conservative or not, for any pair of thermodynamically equidistant temperature quenches warm up faster than they cool down. The relaxation asymmetry [57], which was recently confirmed experimentally [56], therefore persists in driven systems. As the original proof hinged on microscopic reversibility, this finding is surprising and is explained by a nontrivial isomorphism between driven and reversible processes. In the presence of driving a striking feature of the relaxation asymmetry appears: rotational dynamics emerge with opposite directions during heating and cooling, respectively. This further highlights that small, noisy systems do not relax by passing through local equilibria [1]. Moreover, rotations in opposing directions emphasize that heating and cooling evolve along fundamentally distinct pathways [56]. An analysis with the framework of thermal kinematics [56] will bring even deeper insight. Our results motivate further studies on the existence of the relaxation asymmetry in temporally driven systems [49,103–107], systems with nonlinear drift [25,27,28,30,108], and in the presence of inertial effects [35].

Acknowledgments. Financial support from Studienstiftung des Deutschen Volkes (to C.D.) and the Deutsche Forschungsgemeinschaft (DFG, German Research Foundation) through the Emmy Noether Program GO 2762/1-2 (to A.G.) is gratefully acknowledged.

[1] S. R. de Groot and P. Mazur, *Non-equilibrium Thermodynamics*, 2nd ed. (North-Holland, Amsterdam, 1962).
[2] L. Onsager, Reciprocal relations in irreversible processes. I., Phys. Rev. **37**, 405 (1931).
[3] L. Onsager, Reciprocal relations in irreversible processes. II., Phys. Rev. **38**, 2265 (1931).
[4] R. Kubo, M. Yokota, and S. Nakajima, Statistical-mechanical theory of irreversible processes. II. Response to thermal disturbance, J. Phys. Soc. Jpn. **12**, 1203 (1957).
[5] M. Baiesi and C. Maes, An update on the nonequilibrium linear response, New J. Phys. **15**, 013004 (2013).
[6] C. Maes, K. Netočný, and B. Wynants, Monotonic return to steady nonequilibrium, Phys. Rev. Lett. **107**, 010601 (2011).
[7] M. Polettini and M. Esposito, Nonconvexity of the relative entropy for Markov dynamics: A Fisher information approach, Phys. Rev. E **88**, 012112 (2013).
[8] L. Bertini, A. De Sole, D. Gabrielli, G. Jona-Lasinio, and C. Landim, Minimum dissipation principle in stationary nonequilibrium states, J. Stat. Phys. **116**, 831 (2004).
[9] L. Bertini, A. De Sole, D. Gabrielli, G. Jona-Lasinio, and C. Landim, Macroscopic fluctuation theory, Rev. Mod. Phys. **87**, 593 (2015).
[10] R. S. Maier and D. L. Stein, Escape problem for irreversible systems, Phys. Rev. E **48**, 931 (1993).
[11] F. Bouchet and J. Reygner, Generalisation of the Eyring–Kramers transition rate formula to irreversible diffusion processes, Ann. Henri Poincaré **17**, 3499 (2016).
[12] J. Casademunt, R. Mannella, P. V. E. McClintock, F. E. Moss, and J. M. Sancho, Relaxation times of non-Markovian processes, Phys. Rev. A **35**, 5183 (1987).
[13] I. M. Sokolov, Solutions of a class of non-Markovian Fokker-Planck equations, Phys. Rev. E **66**, 041101 (2002).
[14] I. M. Sokolov, Cyclization of a polymer: First-passage problem for a Non-Markovian process, Phys. Rev. Lett. **90**, 080601 (2003).
[15] B. Dybiec, I. M. Sokolov, and A. V. Chechkin, Relaxation to stationary states for anomalous diffusion, Commun. Nonlinear Sci. Numer. Simul. **16**, 4549 (2011).
[16] D. E. Makarov, Interplay of non-Markov and internal friction effects in the barrier crossing kinetics of biopolymers: Insights from an analytically solvable model, J. Chem. Phys. **138**, 014102 (2013).
[17] R. Satija and D. E. Makarov, Generalized Langevin equation as a model for barrier crossing dynamics in biomolecular folding, J. Phys. Chem. B **123**, 802 (2019).
[18] A. Lapolla and A. Godec, Manifestations of projection-induced memory: General theory and the tilted single file, Front. Phys. **7**, 182 (2019).
[19] A. Lapolla and A. Godec, Single-file diffusion in a bi-stable potential: Signatures of memory in the barrier-crossing of a tagged-particle, J. Chem. Phys. **153**, 194104 (2020).
[20] P. Talkner and P. Hänggi, Colloquium: Statistical mechanics and thermodynamics at strong coupling: Quantum and classical, Rev. Mod. Phys. **92**, 041002 (2020).

[21] C. Ayaz, L. Scalfi, B. A. Dalton, and R. R. Netz, Generalized Langevin equation with a nonlinear potential of mean force and nonlinear memory friction from a hybrid projection scheme, Phys. Rev. E **105**, 054138 (2022).

[22] L. F. Cugliandolo, D. S. Dean, and J. Kurchan, Fluctuation-dissipation theorems and entropy production in relaxational systems, Phys. Rev. Lett. **79**, 2168 (1997).

[23] E. Lippiello, M. Baiesi, and A. Sarracino, Nonequilibrium fluctuation-dissipation theorem and heat production, Phys. Rev. Lett. **112**, 140602 (2014).

[24] A. Gal and O. Raz, Precooling strategy allows exponentially faster heating, Phys. Rev. Lett. **124**, 060602 (2020).

[25] Z. Lu and O. Raz, Nonequilibrium thermodynamics of the Markovian Mpemba effect and its inverse, Proc. Natl. Acad. Sci. USA **114**, 5083 (2017).

[26] A. Lasanta, F. Vega Reyes, A. Prados, and A. Santos, When the hotter cools more quickly: Mpemba effect in granular fluids, Phys. Rev. Lett. **119**, 148001 (2017).

[27] M. Baity-Jesi, E. Calore, A. Cruz, L. A. Fernandez, J. M. Gil-Narvión, A. Gordillo-Guerrero, D. Iñiguez, A. Lasanta, A. Maiorano, E. Marinari, V. Martin-Mayor, J. Moreno-Gordo, A. M. Sudupe, D. Navarro, G. Parisi, S. Perez-Gaviro, F. Ricci-Tersenghi, J. J. Ruiz-Lorenzo, S. F. Schifano, B. Seoane *et al.*, The Mpemba effect in spin glasses is a persistent memory effect, Proc. Natl. Acad. Sci. USA **116**, 15350 (2019).

[28] A. Kumar and J. Bechhoefer, Exponentially faster cooling in a colloidal system, Nature (London) **584**, 64 (2020).

[29] F. Carollo, A. Lasanta, and I. Lesanovsky, Exponentially accelerated approach to stationarity in Markovian open quantum systems through the Mpemba effect, Phys. Rev. Lett. **127**, 060401 (2021).

[30] A. Kumar, R. Chétrite, and J. Bechhoefer, Anomalous heating in a colloidal system, Proc. Natl. Acad. Sci. USA **119**, e2118484119 (2022).

[31] I. Klich, O. Raz, O. Hirschberg, and M. Vucelja, Mpemba index and anomalous relaxation, Phys. Rev. X **9**, 021060 (2019).

[32] R. Holtzman and O. Raz, Landau theory for the Mpemba effect through phase transitions, Commun. Phys. **5**, 280 (2022).

[33] J. Degünther and U. Seifert, Anomalous relaxation from a nonequilibrium steady state: An isothermal analog of the Mpemba effect, Europhys. Lett. **139**, 41002 (2022).

[34] I. L. Morgan, R. Avinery, G. Rahamim, R. Beck, and O. A. Saleh, Glassy dynamics and memory effects in an intrinsically disordered protein construct, Phys. Rev. Lett. **125**, 058001 (2020).

[35] A. Militaru, A. Lasanta, M. Frimmer, L. L. Bonilla, L. Novotny, and R. A. Rica, Kovacs memory effect with an optically levitated nanoparticle, Phys. Rev. Lett. **127**, 130603 (2021).

[36] F. Bouchet, K. Gawedzki, and C. Nardini, Perturbative calculation of quasi-potential in non-equilibrium diffusions: A mean-field example, J. Stat. Phys. **163**, 1157 (2016).

[37] Y. Baek and Y. Kafri, Singularities in large deviation functions, J. Stat. Mech. (2015) P08026.

[38] J. P. Garrahan, R. L. Jack, V. Lecomte, E. Pitard, K. van Duijvendijk, and F. van Wijland, Dynamical first-order phase transition in kinetically constrained models of glasses, Phys. Rev. Lett. **98**, 195702 (2007).

[39] T. Speck, A. Engel, and U. Seifert, The large deviation function for entropy production: the optimal trajectory and the role of fluctuations, J. Stat. Mech. (2012) P12001.

[40] P. Tsobgni Nyawo and H. Touchette, A minimal model of dynamical phase transition, Europhys. Lett. **116**, 50009 (2016).

[41] V. Ermolaev and C. Külske, Low-temperature dynamics of the curie-weiss model: Periodic orbits, multiple histories, and loss of gibbsianness, J. Stat. Phys. **141**, 727 (2010).

[42] J. Meibohm and M. Esposito, Finite-time dynamical phase transition in nonequilibrium relaxation, Phys. Rev. Lett. **128**, 110603 (2022).

[43] J. Meibohm and M. Esposito, Landau theory for finite-time dynamical phase transitions, New J. Phys. **25**, 023034 (2023).

[44] K. Blom and A. Godec, Global speed limit for finite-time dynamical phase transition and nonequilibrium relaxation, arXiv:2209.14287.

[45] P. Pietzonka, F. Ritort, and U. Seifert, Finite-time generalization of the thermodynamic uncertainty relation, Phys. Rev. E **96**, 012101 (2017).

[46] A. Dechant and S.-i. Sasa, Current fluctuations and transport efficiency for general Langevin systems, J. Stat. Mech. (2018) 063209.

[47] K. Liu, Z. Gong, and M. Ueda, Thermodynamic uncertainty relation for arbitrary initial states, Phys. Rev. Lett. **125**, 140602 (2020).

[48] T. Koyuk and U. Seifert, Operationally accessible bounds on fluctuations and entropy production in periodically driven systems, Phys. Rev. Lett. **122**, 230601 (2019).

[49] T. Koyuk and U. Seifert, Thermodynamic uncertainty relation for time-dependent driving, Phys. Rev. Lett. **125**, 260604 (2020).

[50] C. Dieball and A. Godec, Direct route to thermodynamic uncertainty relations and their saturation, Phys. Rev. Lett. **130**, 087101 (2023).

[51] N. Shiraishi, K. Funo, and K. Saito, Speed limit for classical stochastic processes, Phys. Rev. Lett. **121**, 070601 (2018).

[52] E. Aurell, C. Mejía-Monasterio, and P. Muratore-Ginanneschi, Optimal protocols and optimal transport in stochastic thermodynamics, Phys. Rev. Lett. **106**, 250601 (2011).

[53] K. Yoshimura and S. Ito, Thermodynamic uncertainty relation and thermodynamic speed limit in deterministic chemical reaction networks, Phys. Rev. Lett. **127**, 160601 (2021).

[54] S. Ito and A. Dechant, Stochastic time evolution, information geometry, and the Cramér-Rao bound, Phys. Rev. X **10**, 021056 (2020).

[55] N. Shiraishi and K. Saito, Information-theoretical bound of the irreversibility in thermal relaxation processes, Phys. Rev. Lett. **123**, 110603 (2019).

[56] M. Ibáñez, C. Dieball, A. Lasanta, A. Godec, and R. A. Rica, Heating and cooling are fundamentally asymmetric and evolve along distinct pathways, arXiv:2302.09061 [Nat. Phys. (to be published)].

[57] A. Lapolla and A. Godec, Faster uphill relaxation in thermodynamically equidistant temperature quenches, Phys. Rev. Lett. **125**, 110602 (2020).

[58] T. V. Vu and Y. Hasegawa, Toward relaxation asymmetry: Heating is faster than cooling, Phys. Rev. Res. **3**, 043160 (2021).

[59] S. K. Manikandan, Equidistant quenches in few-level quantum systems, Phys. Rev. Res. **3**, 043108 (2021).

[60] J. Meibohm, D. Forastiere, T. Adeleke-Larodo, and K. Proesmans, Relaxation-speed crossover in anharmonic potentials, Phys. Rev. E **104**, L032105 (2021).

[61] A. Lapolla and A. Godec, Erratum: Faster uphill relaxation in thermodynamically equidistant temperature quenches [Phys. Rev. Lett. **125**, 110602 (2020)], Phys. Rev. Lett. **128**, 229901(E) (2022).

[62] C.-R. Hwang, S.-Y. Hwang-Ma, and S.-J. Sheu, Accelerating diffusions, Ann. Appl. Probab. **15**, 1433 (2005).

[63] K. S. Turitsyn, M. Chertkov, and M. Vucelja, Irreversible Monte Carlo algorithms for efficient sampling, Phys. D: Nonlinear Phenom. **240**, 410 (2011).

[64] S. C. Kapfer and W. Krauth, Irreversible local Markov chains with rapid convergence towards equilibrium, Phys. Rev. Lett. **119**, 240603 (2017).

[65] L. Rey-Bellet and K. Spiliopoulos, Irreversible Langevin samplers and variance reduction: a large deviations approach, Nonlinearity **28**, 2081 (2015).

[66] F. Coghi, R. Chetrite, and H. Touchette, Role of current fluctuations in nonreversible samplers, Phys. Rev. E **103**, 062142 (2021).

[67] H. Qian, A decomposition of irreversible diffusion processes without detailed balance, J. Math. Phys. **54**, 053302 (2013).

[68] C.-R. Hwang, S.-Y. Hwang-Ma, and S.-J. Sheu, Accelerating Gaussian diffusions, Ann. Appl. Probab. **3**, 897 (1993).

[69] See Supplemental Material at http://link.aps.org/supplemental/10.1103/PhysRevResearch.5.L042030 for further details, derivations, and figures.

[70] J. L. Lebowitz and P. G. Bergmann, Irreversible Gibbsian ensembles, Ann. Phys. (NY) **1**, 1 (1957).

[71] M. C. Mackey, The dynamic origin of increasing entropy, Rev. Mod. Phys. **61**, 981 (1989).

[72] S. Vaikuntanathan and C. Jarzynski, Dissipation and lag in irreversible processes, Europhys. Lett. **87**, 60005 (2009).

[73] M. Esposito and C. Van den Broeck, Three detailed fluctuation theorems, Phys. Rev. Lett. **104**, 090601 (2010).

[74] C. Van den Broeck and M. Esposito, Three faces of the second law. II. Fokker-Planck formulation, Phys. Rev. E **82**, 011144 (2010).

[75] S. Kullback and R. A. Leibler, On information and sufficiency, Ann. Math. Statist. **22**, 79 (1951).

[76] N. Ikeda and S. Watanabe, *Stochastic Differential Equations and Diffusion Processes*, 1st ed. (North Holland, Amsterdam, 1981).

[77] C. W. Gardiner, *Handbook of Stochastic Methods for Physics, Chemistry, and the Natural Sciences* (Springer-Verlag, Berlin, 1985).

[78] C. Dieball and A. Godec, Coarse graining empirical densities and currents in continuous-space steady states, Phys. Rev. Res. **4**, 033243 (2022).

[79] U. Seifert, Stochastic thermodynamics, fluctuation theorems and molecular machines, Rep. Prog. Phys. **75**, 126001 (2012).

[80] B. H. Zimm, Dynamics of polymer molecules in dilute solution: Viscoelasticity, flow birefringence and dielectric loss, J. Chem. Phys. **24**, 269 (1956).

[81] M. Doi and S. F. Edwards, *The Theory of Polymer Dynamics*, International Series of Monographs on Physics (Clarendon Press, Oxford, 1988).

[82] R. R. Cheng, A. T. Hawk, and D. E. Makarov, Exploring the role of internal friction in the dynamics of unfolded proteins using simple polymer models, J. Chem. Phys. **138**, 074112 (2013).

[83] A. Soranno, B. Buchli, D. Nettels, R. R. Cheng, S. Müller-Späth, S. H. Pfeil, A. Hoffmann, E. A. Lipman, D. E. Makarov, and B. Schuler, Quantifying internal friction in unfolded and intrinsically disordered proteins with single-molecule spectroscopy, Proc. Natl. Acad. Sci. USA **109**, 17800 (2012).

[84] B. Schuler, A. Soranno, H. Hofmann, and D. Nettels, Single-molecule FRET spectroscopy and the polymer physics of unfolded and intrinsically disordered proteins, Annu. Rev. Biophys. **45**, 207 (2016).

[85] J. O. Daldrop, J. Kappler, F. N. Brünig, and R. R. Netz, Butane dihedral angle dynamics in water is dominated by internal friction, Proc. Natl. Acad. Sci. USA **115**, 5169 (2018).

[86] D. E. Smith, H. P. Babcock, and S. Chu, Single-polymer dynamics in steady shear flow, Science **283**, 1724 (1999).

[87] S. Gerashchenko and V. Steinberg, Statistics of tumbling of a single polymer molecule in shear flow, Phys. Rev. Lett. **96**, 038304 (2006).

[88] P. S. Doyle, B. Ladoux, and J.-L. Viovy, Dynamics of a tethered polymer in shear flow, Phys. Rev. Lett. **84**, 4769 (2000).

[89] T. T. Perkins, D. E. Smith, R. G. Larson, and S. Chu, Stretching of a single tethered polymer in a uniform flow, Science **268**, 83 (1995).

[90] C. M. Schroeder, R. E. Teixeira, E. S. G. Shaqfeh, and S. Chu, Characteristic periodic motion of polymers in shear flow, Phys. Rev. Lett. **95**, 018301 (2005).

[91] R. E. Teixeira, H. P. Babcock, E. S. G. Shaqfeh, and S. Chu, Shear thinning and tumbling dynamics of single polymers in the flow-gradient plane, Macromolecules **38**, 581 (2005).

[92] M. Harasim, B. Wunderlich, O. Peleg, M. Kröger, and A. R. Bausch, Direct observation of the dynamics of semiflexible polymers in shear flow, Phys. Rev. Lett. **110**, 108302 (2013).

[93] A. Alexander-Katz, M. F. Schneider, S. W. Schneider, A. Wixforth, and R. R. Netz, Shear-flow-induced unfolding of polymeric globules, Phys. Rev. Lett. **97**, 138101 (2006).

[94] T. T. Perkins, D. E. Smith, and S. Chu, Single polymer dynamics in an elongational flow, Science **276**, 2016 (1997).

[95] Y. Roichman, B. Sun, A. Stolarski, and D. G. Grier, Influence of nonconservative optical forces on the dynamics of optically trapped colloidal spheres: The fountain of probability, Phys. Rev. Lett. **101**, 128301 (2008).

[96] G. Metafune, L^p-spectrum of Ornstein-Uhlenbeck operators, Ann. Scuola Norm. Sup. Pisa Cl. Sci. **30**, 97 (2001).

[97] G. Metafune, D. Pallara, and E. Priola, Spectrum of Ornstein-Uhlenbeck operators in l^p spaces with respect to invariant measures, J. Funct. Anal. **196**, 40 (2002).

[98] H. F. Trotter, On the product of semi-groups of operators, Proc. Amer. Math. Soc. **10**, 545 (1959).

[99] T. Hatano and S.-i. Sasa, Steady-state thermodynamics of Langevin systems, Phys. Rev. Lett. **86**, 3463 (2001).

[100] A. Dechant and S.-i. Sasa, Continuous time reversal and equality in the thermodynamic uncertainty relation, Phys. Rev. Res. **3**, L042012 (2021).

[101] C. Dieball and A. Godec, Mathematical, thermodynamical, and experimental necessity for coarse graining empirical densities and currents in continuous space, Phys. Rev. Lett. **129**, 140601 (2022).

[102] G. Dahlquist, *Stability and Error Bounds in the Numerical Integration of Ordinary Differential Equations* (Almqvist & Wiksell, Uppsala, 1958).

[103] V. Blickle and C. Bechinger, Realization of a micrometre-sized stochastic heat engine, Nature Phys. **8**, 143 (2012).

[104] I. A. Martínez, É. Roldán, L. Dinis, D. Petrov, and R. A. Rica, Adiabatic processes realized with a trapped Brownian particle, Phys. Rev. Lett. **114**, 120601 (2015).

[105] I. A. Martínez, É. Roldán, L. Dinis, D. Petrov, J. M. R. Parrondo, and R. A. Rica, Brownian Carnot engine, Nature Phys. **12**, 67 (2016).

[106] S. Krishnamurthy, S. Ghosh, D. Chatterji, R. Ganapathy, and A. K. Sood, A micrometre-sized heat engine operating between bacterial reservoirs, Nature Phys. **12**, 1134 (2016).

[107] M. Rademacher, M. Konopik, M. Debiossac, D. Grass, E. Lutz, and N. Kiesel, Nonequilibrium control of thermal and mechanical changes in a levitated system, Phys. Rev. Lett. **128**, 070601 (2022).

[108] J. Gladrow, M. Ribezzi-Crivellari, F. Ritort, and U. F. Keyser, Experimental evidence of symmetry breaking of transition-path times, Nature Commun. **10**, 55 (2019).